JMEPEG (2012) 21:1978–1988
DOI: 10.1007/s11665-011-0105-z
©ASM International
1059-9495/$19.00

Optimization of Experimental Conditions of the Pulsed Current GTAW Parameters for Mechanical Properties of SDSS UNS S32760 Welds Based on the Taguchi Design Method

M. Yousefieh, M. Shamanian, and A. Saatchi

(Submitted March 1, 2011; in revised form July 10, 2011)

Taguchi design method with L_9 orthogonal array was implemented to optimize the pulsed current gas tungsten arc welding parameters for the hardness and the toughness of super duplex stainless steel (SDSS, UNS S32760) welds. In this regard, the hardness and the toughness were considered as performance characteristics. Pulse current, background current, % on time, and pulse frequency were chosen as main parameters. Each parameter was varied at three different levels. As a result of pooled analysis of variance, the pulse current is found to be the most significant factor for both the hardness and the toughness of SDSS welds by percentage contribution of 71.81 for hardness and 78.18 for toughness. The % on time (21.99%) and the background current (17.81%) had also the next most significant effect on the hardness and the toughness, respectively. The optimum conditions within the selected parameter values for hardness were found as the first level of pulse current (100 A), third level of background current (70 A), first level of % on time (40%), and first level of pulse frequency (1 Hz), while they were found as the second level of pulse current (120 A), second level of background current (60 A), second level of % on time (60%), and third level of pulse frequency (5 Hz) for toughness. The Taguchi method was found to be a promising tool to obtain the optimum conditions for such studies. Finally, in order to verify experimental results, confirmation tests were carried out at optimum working conditions. Under these conditions, there were good agreements between the predicted and the experimental results for the both hardness and toughness.

Keywords ANOVA, hardness, optimization, pulse current GTAW, Taguchi method, toughness

1. Introduction

Super duplex stainless steels (SDSS) are iron-based alloys consisting of two phases: ferrite (α) and austenitic (γ). The α/γ ratio is typically 50:50 (Ref 1). The fine austenite-ferrite microstructure of these materials promotes an excellent combination of toughness and mechanical strength, desirable for many applications in the chemical and petrochemical industries (Ref 2).

During welding operations, the main concern is to obtain austenite contents close to 50% and to avoid the formation of deleterious phases such as sigma (σ) and Cr_2N during cooling and re-heating passes (Ref 3). Typically, the σ phase and the hexagonal nitrides (Cr_2N) are precipitated in a temperature range of 600-1000 and 700-900 °C, respectively. The considerable presence of precipitates such as Cr_2N and σ phase can deteriorate corrosion and mechanical properties. Therefore, enormous heat inputs should be avoided to minimize the risk of precipitation of σ and other intermetallic phases. On the other hand, low heat inputs should also be avoided to minimize the risk of precipitating too high ferrite content and the precipitation of Cr_2N (Ref 4). Therefore, welding specifications must be designed to obtain phase proportions (ferrite/austenite ratio) near 1:1 and to avoid σ and Cr_2N precipitation (Ref 5, 6). In this case, the cooling time in the range of 1200-800 °C (the range of austenite formation), viz., $\Delta t_{12/8}$, is a key welding parameter for SDSS.

Pulsed current gas tungsten arc welding (PCGTAW) is a joining technology, which is a variant of the constant current gas tungsten arc welding (CCGTAW) process which is used in a wide range of industrial applications (Ref 7). The PCGTAW involves cycling of the welding current from a high level to a low level at a selected regular frequency. The high level of the pulse current is generally selected to give adequate penetration and bead contour, while the low level of the background current is set at a level sufficient to improve stability of arc. The PCGTAW process has a numerous advantages over the constant current GTAW process. The beneficial effects most often reported in the literature are (1) refined grain size, (2) low distortion, (3) enhanced arc stability, (4) reduced porosity, (5) increased weld depth to width ratio, (6) reduction in the heat-affected zone (HAZ), and (7) better control of heat input (Ref 6, 8). In general, the pulsed current GTAW process is suitable for joining thin and medium thickness materials, e.g., stainless steel sheets, and for applications where metallurgical control of the weld metal is critical (Ref 9). All these advantages will help

M. Yousefieh, M. Shamanian, and **A. Saatchi**, Department of Materials Engineering, Isfahan University of Technology, 84156-83111 Isfahan, Iran. Contact e-mails: m.yousefieh@ma.iut.ac.ir and shamanian@cc.iut.ac.ir.

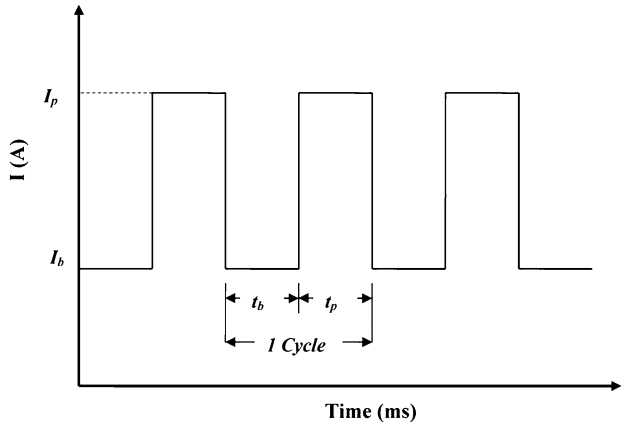

Fig. 1 Pulsed current GTAW process parameters. I_p is the pulse current, A; I_b is the background current, A; t_p is the pulse current duration, ms; t_b background is the current duration, ms; $F = 1/(t_p + t_b)$ is the pulse frequency, Hz; % on time is the pulse current duration in one cycle

in improving mechanical and corrosion properties. The definitions of pulse current, background current, and time duration modes are schematically illustrated in Fig. 1.

The authors have investigated earlier the effect of PCGTAW parameters on the corrosion resistance of SDSS UNS S32760 welds (Ref 6). But, reported research works related to the effect of pulsed current parameters on mechanical properties are very scanty. Moreover, no systematic study has been reported so far to analyze the influence of pulsed current parameters on mechanical properties such as toughness and hardness.

Taguchi method was developed as a process optimization technique by Genichi Taguchi during the 1950s (Ref 10). Taguchi's approach provides the design engineer with a systematic and efficient method for determining near-optimum design parameters for performance and cost. In addition to keep the experimental cost at the minimum level, another advantage of the Taguchi method is the minimization of the variability around the target when the performance value is close to the target value. In addition, the optimum working conditions determined from the laboratory work can be reproduced in the real production environment (Ref 10, 11). Various steps of Taguchi method are shown in Fig. 2 (Ref 6, 12).

The specific objective of this investigation is to study the methodological application of Taguchi orthogonal array (OA) experimental design (DOE) to optimize the pulsed GTAW process parameters to improve the mechanical properties such as toughness and hardness of SDSS UNS S32760 welds. Moreover, this current research will be useful to select suitable welding process parameters to control the heat input and cooling rates during welding such that the mechanical properties of the weld could be improved.

2. Experimental Procedures

A 5 mm thick, 500 mm diameter pipe of super duplex UNS S32760 stainless steel was welded using PCGTAW process with ER 2594 filler metal. The detail of the welding parameters is given as follows:

Arc plasma and shielding gas: High-purity argon (99.99% pure), flow rate (L/min): 10

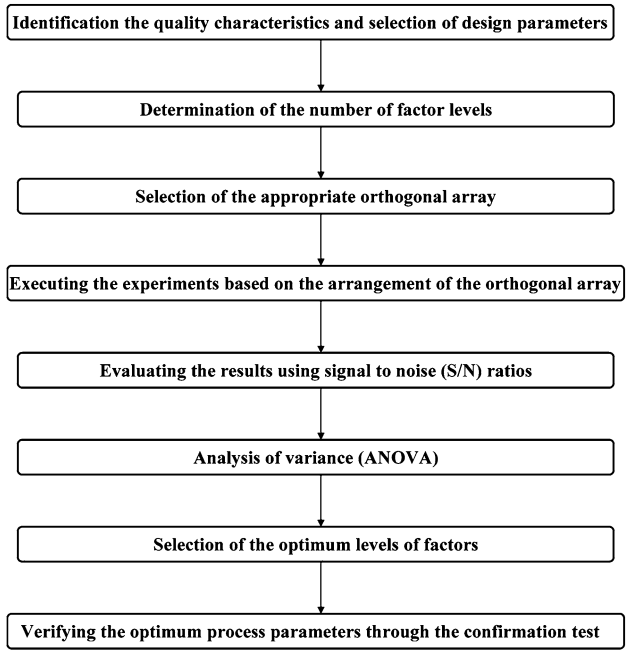

Fig. 2 Various steps of Taguchi method

Electrode: ER 2594 (AWS)
Voltage: 15 V
Travel speed: 10 cm/min.

The chemical composition of the base and filler materials used in this study is given in Table 1.

In CCGTAW process, heat input is calculated from constant current, whereas in the PCGTAW process, heat input is calculated from the mean current (I_m). The equation for mean current (Ref 6, 9) may be given as:

$$I_m = \frac{I_p \times t_p + I_b \times t_b}{t_p + t_b} \text{ (A)} \quad \text{(Eq 1)}$$

Heat input (HI) is calculated using following equation (Ref 6, 9):

$$HI = \eta \times \frac{I_m \times V}{S} \text{ (kJ/mm)} \quad \text{(Eq 2)}$$

I_p is the pulse current, A; I_b is the background current, A; t_b background is the current duration, ms; t_p is the pulse current duration, ms; S is the welding speed, cm/min; V is the voltage, V; η is the efficiency of the welding process.

For the PCGTAW process, arc efficiency is taken as 60% (Ref 6, 9).

The microstructural investigations were carried out on samples prepared from the weldments. In order to reveal the σ phase and eventually Cr_2N that precipitated in association with σ (Ref 6, 13, 14), the samples were electrolytically etched using a KOH solution (100 mL H_2O + 15 g of potassium hydroxide) at an etching potential of 3 V for 12 s. A number of samples were electrolytically etched with a solution containing 10% oxalic acid at an etching potential of 8 V for 50 s to reveal Cr_2N in the ferrite (Ref 6).

Ferrite content of polished and etched specimens was measured using a Fischer ferritescope calibrated according to IIW secondary standards. Moreover, the austenite content was measured using x-ray diffractometry (XRD) (Ref 15). In this

Table 1 Nominal chemical composition of materials used (wt.%)

Element	C	Mn	P	S	Si	Cr	Ni	Mo	N	Cu
Base metal (UNS S32760)	0.03	0.82	0.02	0.01	0.93	25.7	6.3	3.4	0.23	0.61
Filler metal (ER 2594)	0.03	0.73	0.001	0.002	0.94	25.9	9.2	4.2	0.22	0.54

Table 2 Process parameters and design levels used in experiments

Character	Parameters	Units	Level 1	Level 2	Level 3
A	Pulse current	Ampere (A)	100	120	140
B	Background current	Ampere (A)	50	60	70
C	% On time	…	40	60	80
D	Pulse frequency	Hertz (Hz)	1	3	5

regard, samples were analyzed by XRD (Philips X'Pert-MPD) using Cu-Kα radiation (λ = 1.54056 Å) generated at 40 kV and 30 mA. X'Pert software was used for analysis of diffractograms.

The microstructures and fracture surfaces of samples were investigated using a scanning electron microscope (SEM) equipped with an energy dispersive x-ray spectrometer (EDX) for chemical analysis. The x-ray count rate was estimated as 2×10^3 counts per second (cps).

The Charpy-V reduced size samples (2.5 mm) were machined according to the ASTM E23 standard (Ref 16). The Charpy tests were carried out at room temperature. The Vickers hardness measurements were performed at a load of 30 kgf.

3. Taguchi Design of Experiment (DOE)

Taguchi method is a systematic application of design and analysis of experiments for the purpose of designing and improving product quality. The Taguchi method uses a special of OAs to study all the designed factors with a minimum of experiments. Orthogonality means that each factor is independently evaluated and the effect of one factor does not interfere with the estimation of the influence of another factor (Ref 17, 18).

Table 2 shows the key four PCGTAW process parameters investigated at the three experimental levels. In the next step, matrix was designed with the appropriate OAs for the selected parameters and their levels. Taguchi provides many standard OAs and corresponding linear graphs for this purpose.

The OA experimental design method was chosen to determine experimental plan, L_9 (3^4) (Table 3), because it is the most suitable for the conditions being investigated; four parameters each with three values (Ref 19). The L_9 (3^4) (which indicated 9 experimental trials) is one of the standard orthogonal experimental plans of Taguchi. The order of the experiments was obtained by inserting parameters into the columns of the OA, L_9 (3^4), chosen as the experimental plan given in Table 3, but the order of experiments was made random to avoid noise sources which had not been considered initially and which could take place during an experiment and affect the results in a negative way.

Taguchi method recommends the signal-to-noise (S/N) ratio, which is a performance characteristic, instead of the average value. Optimum conditions were determined using the S/N ratio

Table 3 Experimental layout using L_9 (3^4) OA

	Factors			
Trial no.	A	B	C	D
1	1	1	1	1
2	1	2	2	2
3	1	3	3	3
4	2	1	2	3
5	2	2	3	1
6	2	3	1	2
7	3	1	3	2
8	3	2	1	3
9	3	3	2	1

of experimental results (Ref 6). There are three S/N ratios of common interest for the optimization of static problem, the higher the better (HB), the lower the better (LB), and the nominal the better (NB). The larger S/N ratio respects to better performance characteristic.

Then the mean S/N ratios at each level for various factors must be calculated. Moreover, the optimal level, that is the largest S/N ratio among all the levels of the factors, can be determined. A statistical analysis of variance (ANOVA) was also performed to indicate which process parameters are statistically significant; the optimal combination of the process parameters can then be reproduced.

In order to validate the methodology, confirmation experiments must be performed at optimal process parameters to verify predicted results. If the predicted results are confirmed, the suggested optimum working conditions will be adopted (Ref 12).

4. Results and Discussion

4.1 Taguchi Results

In this study, an L_9 (3^4) OA with 4 columns and 9 rows was used. This array can handle three-level process parameters. Nine experiments were necessary to study the welding parameters using the L_9 (3^4) OA. In order to evaluate the influence of each selected factor on the responses, the S/N ratios for each control factor had to be calculated.

In the Taguchi method, the terms "signal" and "noise" represent the desirable and undesirable values for the output characteristic, respectively. Taguchi method uses the S/N ratio to measure the quality characteristic deviating from the desired value. The S/N ratios are different according to the type of characteristic.

Suitable S/N ratio must be chosen using previous knowledge, expertise, and understanding of the process. When the target is fixed and there is a trivial or absent signal factor (static design), it is possible to choose the S/N ratio depending on the goal of the design.

As mentioned earlier, there are three categories of quality characteristics, i.e., HB, LB, and NB. The performance statistics were chosen as the optimization criterion. In this study, hardness and toughness are treated as a characteristic value. Since the hardness and the toughness welds intended to be maximized, they were both used for "HB" situations, evaluated using the following equation (Ref 6, 12):

$$S/N = -10\log_{10}\left(\frac{1}{n}\sum_{i=1}^{n}\frac{1}{Y_i^2}\right) \quad \text{(Eq 3)}$$

where S/N are performance statistics, defined as the signal-to-noise ratio (S/N unit: dB), n the number of repetitions for an experimental combination, and Y_i a performance value of the ith experiment. Table 4 shows the experimental results for hardness and toughness and the corresponding S/N ratios using Eq 3. Moreover, the calculated heat inputs and austenite contents for each series of experiments are presented in Table 4.

As shown in Table 4, the total mean S/N ratio for hardness is η_m = (total S/N ratio)/(number of experimental runs) = 49.2047 dB. In the similar way, the total mean S/N ratio for toughness was calculated as 33.2959 dB.

Since the experimental design is orthogonal, it is then possible to separate out the effect of each parameter at the different levels (Ref 20). In fact, average performance (mean S/N ratio) of a factor at certain level is the influence of the factor at this level on the mean response of the experiments. In the case of hardness, to compute the average performance of the factor C at level 2 (denoted as C_2), results for trials including factor C_2 were added and then divided by the number of such trials:

$$C_2 = (S/N_2 + S/N_4 + S/N_9)/3 = \left[(49.4258) + (47.7833) + (49.0050)\right]/3 = 48.7380$$

The mean S/N ratio for each level of the other parameters can be calculated in the same way. The mean S/N ratio for each level of the parameters is summarized and the S/N response table for hardness is shown in Table 5.

The rank 1 in Table 5 indicates that pulse current (1) has more significant effect on the hardness followed by rank (2) % on time, which has lesser effect, while ranks (3) and (4) have minimum or no effect on the hardness.

Figure 3 shows the S/N response graph for hardness. As seen in Fig. 3, pulse current and % on time exhibit large variations. The variations are found to be small in the cases of background current and pulse frequency. In other words, background current and pulse frequency to be less effective than those of other parameters, whereas pulse current and % on time are found to be much more effective. Also it can be seen from Fig. 3 that the slopes of the lines between the different levels are not the same for pulse current and % on time factors. So, the levels have different influences on hardness. However, the slopes of the lines are almost the same for background current and pulse frequency.

Figure 3(a) shows the response of the S/N ratio to pulse current for hardness. It can be seen from Fig. 3(a) that the mean S/N ratio drops to the bottom of the curve as the pulse current increases to 120 A from 100 A. When the pulse current increases to 140 A, the mean S/N ratio bounces back upward. The response of the S/N ratio to the % on time, Fig. 3(c), is similar to that for the pulse current. The mean S/N ratio decreases at first as the % on time increases from 40 to 60. The

Table 4 Experimental results for hardness and toughness and corresponding S/N ratios, heat inputs, and austenite contents

Trial no.	Pulse current, A	Background current, A	% on time	Pulse frequency, Hz	Hardness, HV	S/N ratio, dB	Toughness, J	S/N ratio, dB	Heat input, kJ/mm	Austenite content, %
1	100	50	40	1	326	50.2644	39	31.8213	0.630	25
2	100	60	60	3	296	49.4258	47	33.4420	0.763	33
3	100	70	80	5	312	49.8831	44	32.8691	0.846	37
4	120	50	60	3	245	47.7833	52	34.3201	0.955	41
5	120	60	80	5	273	48.7233	56	34.9638	0.756	32
6	120	70	40	1	276	48.8182	53	34.4855	0.900	39
7	140	50	80	5	299	49.5134	40	32.0412	0.936	40
8	140	60	40	1	296	49.4258	46	33.2552	1.116	49
9	140	70	60	3	282	49.0050	42	32.4650	0.890	39
Average						49.2047		33.2959		

Table 5 S/N response table for hardness

Parameters	Character	Level 1	Level 2	Level 3	Delta (Δ) = maximum − minimum	Rank
Pulse current, A	A	**49.8578**	48.4416	49.3147	1.4162	1
Background current, A	B	49.1870	49.1916	**49.2354**	0.0484	4
% On time	C	**49.5028**	48.7380	49.3733	0.7647	2
Pulse frequency, Hz	D	**49.3309**	49.2525	49.0307	0.3001	3

The optimum levels of the factors are given in bold (the highest value in the row)

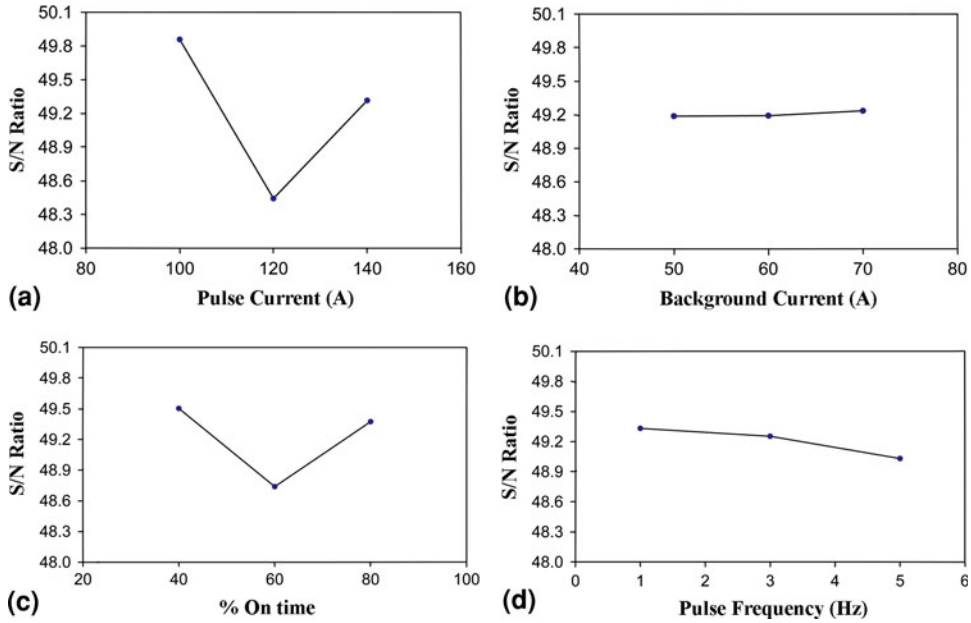

Fig. 3 The S/N response graph for hardness to: (a) pulse current, (b) background current, (c) % on time, and (d) pulse frequency

S/N ratio then increases as the % on time, increases to 80. The highest hardness occurred at lowest pulse current (100 A) and % on time (40), which is the first pulse current and % on time values among the three levels tested in this study. This may be due to the Cr_2N precipitation and excess ferrite phase; this is in agreement with the results of Tavares et al. (Ref 2) in a duplex stainless steel UNS S31803, and Chen and Yang (Ref 21) in a nitrogen-containing 2205 duplex stainless steel.

Figure 3(b), (d) shows the response of the S/N ratio to the background current and pulse frequency for hardness. The slopes of the lines between the three levels are almost the same. It can be seen from Fig. 3(b), (d) that the background current and pulse frequency are insignificant; however, their slopes are opposite to each other. This indicates an interaction between background current and pulse frequency on hardness. While one of them increases the hardness at the same level, the other decreases.

As shown in Eq 3, the greater is the S/N ratio, the smaller is the variance of hardness around the desired (HB) value (Ref 20). In Table 5, A1, B3, C1, and D1 illustrate the largest values of S/N ratios for factors A, B, C, and D, respectively. In other words, based on the S/N ratio, the optimal parameters (conditions) for hardness are A at level 1, B at level 3, C at level 1 and D at level 1, as given in Table 6.

The S/N response table and graph for toughness are shown in Table 7 and Fig. 4, respectively. It was found that the values (Delta (Δ) = maximum – minimum) of pulse current ($\Delta = 2.0027$) and background current ($\Delta = 1.1594$) are higher than any other factors, implying that these parameters have the most significant influence. The effects of pulse frequency ($\Delta = 0.3981$) and % on time ($\Delta = 0.2217$) are less important when compared to the other factors. Consequently, the hardness and the toughness of SDSS welds were all mainly affected by the pulse current.

As shown in Fig. 4, the slopes of the lines between the different levels are not the same for pulse current, background current and % on time factors while the slopes of the lines are almost the same for pulse frequency. According to this figure,

Table 6 Optimum working conditions for hardness and toughness

	Hardness		Toughness	
Parameters	**Level**	**Values**	**Level**	**Values**
Pulse current, A	1	100	2	120
Background current, A	3	70	2	60
% On time	1	40	2	60
Pulse frequency, Hz	1	1	3	5

while pulse current is the most effective parameter, the % on time is the least effective. Consequently, when Fig. 4 is inspected, it can be seen that the effect of the factors on toughness is given in rank, starting with the most effective: pulse current, background current, pulse frequency and % on time.

The responses of the S/N ratio to pulse current and background current are shown in Fig. 4(a), (b). The mean S/N ratio goes up until it reaches a peak at the pulse current of 120 A. After that, the mean S/N ratio decreases with increase of pulse current to 140 A. The response of the S/N ratio to the background current, Fig. 4(b), is alike to that for the pulse current. It can be seen from Fig. 4(a) and (b) that the pulse current and the background current of maximum toughness were observed at 120 and 60 A, respectively, which are the medium values among the three levels tested in this study. The observation on the response of the S/N ratio to pulse current and background current may be mainly due to the precipitate of the intermetallic phases such as σ and Cr_2N. In fact, the formation of intermetallic phases leads to a disastrous loss of toughness (Ref 2, 22). Moreover, the toughness may be affected by the austenite and the σ contents (Ref 22, 23).

Figure 4(c), (d) shows the responses of the S/N ratio to % on time and pulse frequency, respectively. It can be seen from these figures that % on time and pulse frequency are insignificant.

Table 7 S/N response table for toughness

Parameters	Character	Level 1	Level 2	Level 3	Delta (Δ) = maximum − minimum	Rank
Pulse current, A	A	32.7108	**34.5898**	32.5871	2.0027	1
Background current, A	B	32.7275	**33.8870**	33.2732	1.1594	2
% On time	C	33.1873	**33.4090**	33.2913	0.2217	4
Pulse frequency, Hz	D	33.0833	33.3229	**33.4814**	0.3981	3

The optimum levels of the factors are given in bold (the highest value in the row)

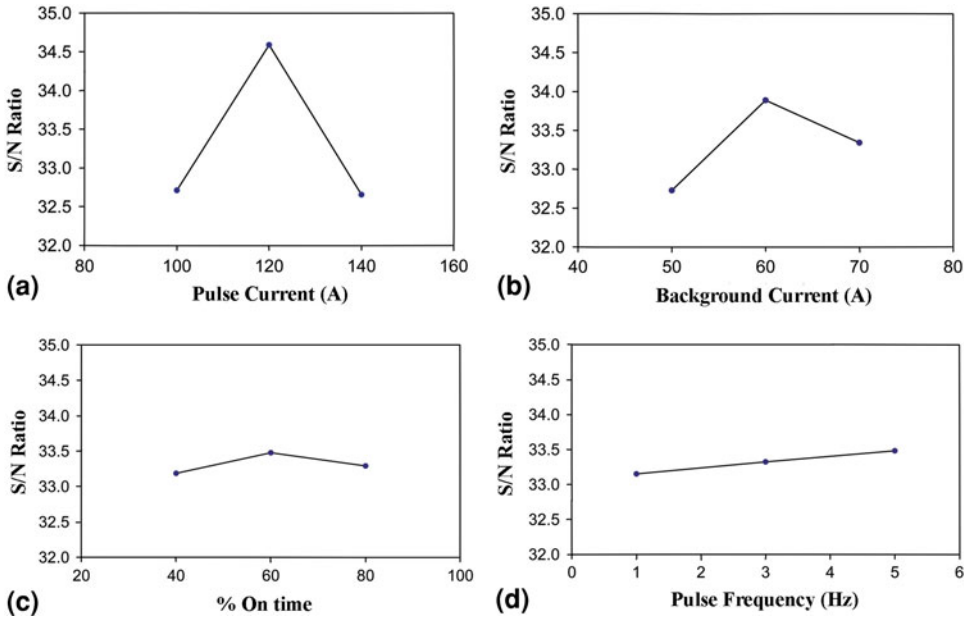

Fig. 4 The S/N response graph for toughness to: (a) pulse current, (b) background current, (c) % on time, and (d) pulse frequency

Since the effects of % on time and pulse frequency on the toughness is not remarkable, these factors may be used with the intention of evaluating the waste.

In the case of toughness, the optimal conditions are A2, B2, C2, and D3 (see Table 7). Restated, the pulse current is 120 A, background current is 60 A, % on time is 60, and pulse frequency is 5 Hz, as given in Table 6.

Figure 5 shows the microstructure of weld metal at trial no. 1 conditions which showed the highest hardness (326 HV) and lowest toughness (39 J). As shown in this figure, chromium nitride (Cr_2N) precipitation is prone to occur in the ferrite domains, due to low solubility of nitrogen in this phase. Moreover, at this condition, the austenite content was very small; consequently, a high level of the ferrite phase was present in this region (at average 68%), which favors the nitrogen segregation in the ferrite phase and the precipitation of Cr_2N on cooling (Ref 2). Indeed, the high ferrite content in this sample (trial no. 1) is due to the low heat input (0.630 kJ/mm) and rapid solidification ($\Delta t_{12/8}$ = 7 s) under these conditions that impedes nitrogen migration to austenite. The Cr_2N precipitation and excess content of body centered cubic (bcc) ferrite phase contribute to the poor toughness (39 J) and higher hardness (326 HV) of this sample (Ref 2, 22, 24).

Moreover, the Charpy test fracture surface of this sample (trial no. 1) was examined by SEM, as shown in Fig. 6. As mentioned earlier, the microstructure of this sample is composed

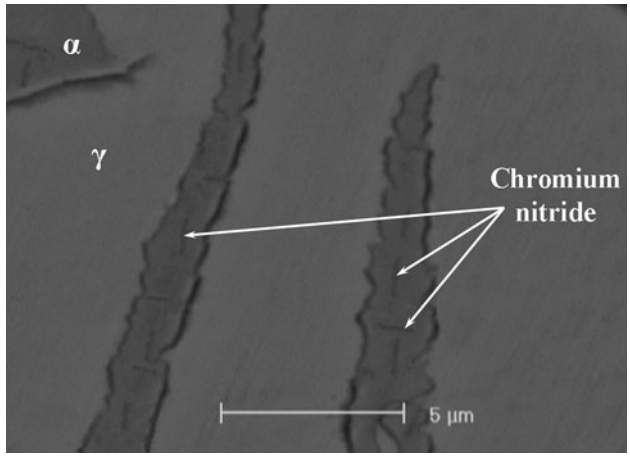

Fig. 5 SEM micrograph from UNS S32760 sample welded at trial no. 1 conditions

of the high ferrite content (68%) and the Cr_2N precipitation that produce a very brittle structure. In this case, the fractograph exhibits regions of cleavage fracture.

Figure 7 shows the microstructure of weld metal at trial no. 8 showing intermediate hardness (296 HV) and toughness (46 J). As shown in Fig. 7, the microstructure is characterized by a high

amount of the σ phase at the ferrite/austenite interfaces. Table 8 shows the concentrations of major alloying elements in the ferrite, the austenite, and the σ phases obtained from EDX analysis of the sample welded at trial no. 8. In Fe-Cr-Ni systems, the σ phase has an Fe-Cr composition and a tetragonal crystalline structure with 30 atoms per unit cell (Ref 25, 26). It is also observed that the ferrite is richer in Cr and Mo while the austenite phase is slightly richer in Ni and Mn. The austenite-to-ferrite ratio increases as a function of increased heat input. A large amount of ferrite has transformed to austenite on cooling at these conditions ($HI_{\text{trial no. 8}}$ = 1.116 kJ/mm). The austenite and the σ contents of this sample were measured and found to be about 49 and 31%, respectively. As shown in Fig. 7, the high austenite and σ contents are due to the high heat input (1.116 kJ/mm) and slow cooling rate ($\Delta t_{12/8}$ = 17 s) under these conditions. This sample (trial no. 8) exhibited intermediate hardening due to the increased concentration of the σ phase in the microstructure. On the other hand, the toughness is negatively affected by the formation of intermetallic phases such as σ. This is due to the bad deformability of the σ phase because of its low fraction or metallic binding (Ref 23). Moreover, the fractographic examination of this sample (trial no. 8) (Fig. 8) shows the brittle areas, due to the presence of the σ phase in the microstructure.

Figure 9 shows the microstructure of weld metal at trial no. 4 exhibiting the lowest hardness (245 HV) and high toughness (52 J). The EDX analysis (Table 8) and SEM observation have shown somewhat trace of the σ phase in the ferrite/austenite interfaces. The austenite and σ contents of this sample were 41 and 6.3%, respectively. This is due to the mediocre heat input (0.955 kJ/mm) and cooling rate ($\Delta t_{12/8}$ = 12 s) under these conditions. The initial stages of the σ phase formation apparently do not increase the hardness; this is in agreement with the results of Moura et al. (Ref 27) in a duplex stainless steel UNS S31803, and Nilssom et al. (Ref 28) in a super duplex steel. In the case of toughness, the cooling rate of super duplex welds must be high enough to obtain at least 35% of austenite and fast enough to reduce the σ phase precipitation. Hence, the high toughness (52 J) of this sample is due to the high austenite content and the low σ precipitation. Moreover, the fracture surface of this sample presented a mixture of brittle and ductile fracture (Fig. 10). Consequently, the surface of this sample is composed of regions of cleavage fracture and plastic deformation.

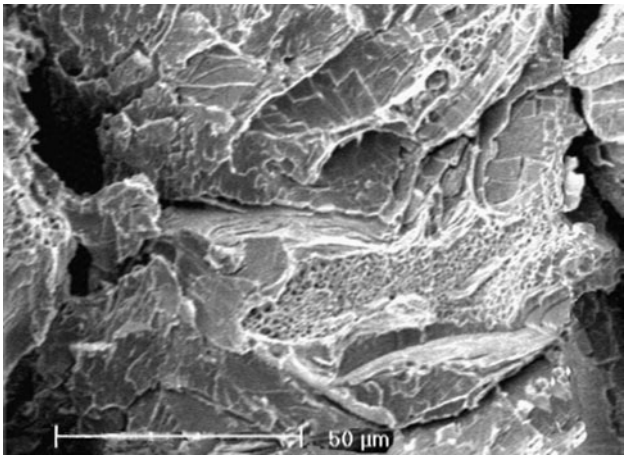

Fig. 6 SEM micrograph from fracture surface of Charpy impact sample welded at trial no. 1

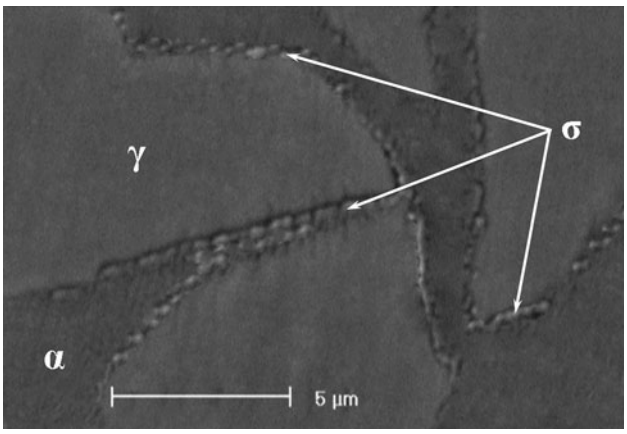

Fig. 7 SEM micrograph from UNS S32760 sample welded at trial no. 8

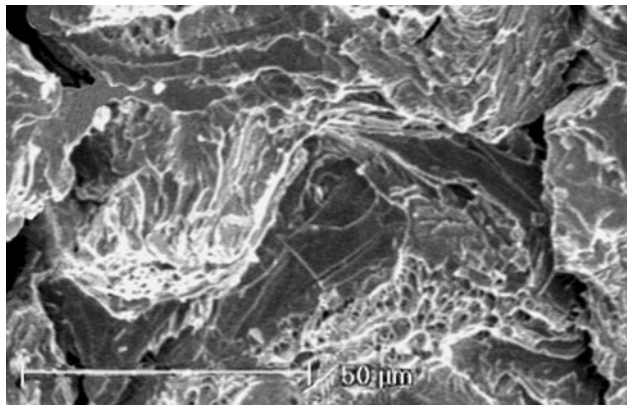

Fig. 8 SEM micrograph from fracture surface of Charpy impact sample welded at trial no. 8

Table 8 Chemical composition of σ and matrix phases determined by energy dispersive x-ray spectrometer analysis (wt.%)

	Element			
Phase	**Chromium**	**Molybdenum**	**Nickel**	**Iron**
γ	25.36	3.29	8.64	62.71
α	27.86	4.72	5.81	61.61
σ (in the microstructure of trial no. 8)	32.62	9.51	5.36	52.51
σ (in the microstructure of trial no. 4)	30.24	8.48	5.17	56.11

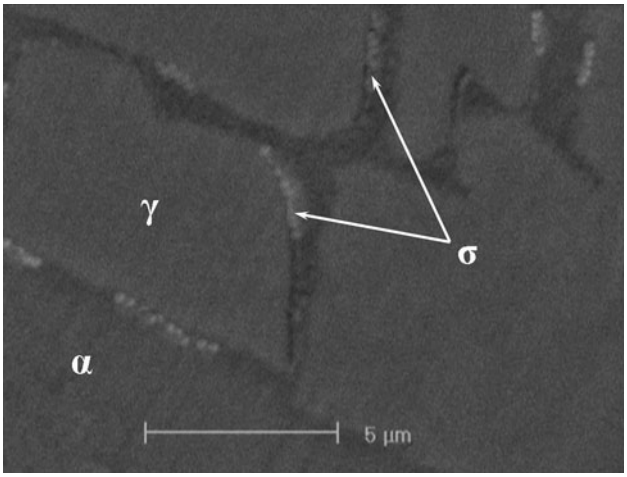

Fig. 9 SEM micrograph from UNS S32760 sample welded at trial no. 4

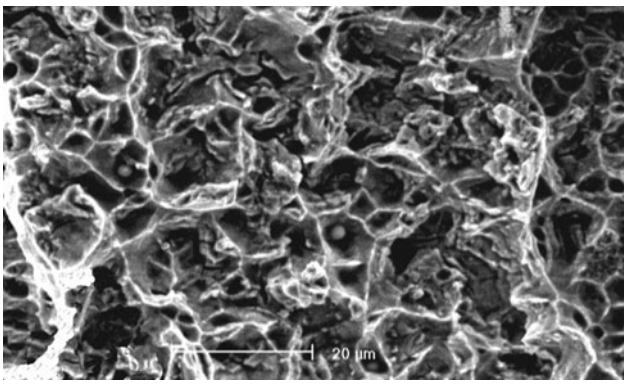

Fig. 10 SEM micrograph from fracture surface of Charpy impact sample welded at trial no. 4

4.2 ANOVA Results

The knowledge of the contribution of individual factors is critically important for the control of the final response. The ANOVA is a common statistical technique to determine the percent contribution of each factor for results of the experiment (Ref 29). It calculates parameters known as sum of squares (SS), corrected sum of squares (SS′), degree of freedom (D), variance (V), and percentage of the contribution of each factor (P). Since the procedure of ANOVA is very complicated and employs a considerable of statistical formulae, only a brief description is given as follows (Ref 6, 30):

$$\mathrm{SS_T} = \sum_{i}^{m} \eta_i^2 - \frac{1}{m}\left[\sum_{i=1}^{m} \eta_i\right]^2 \quad \text{(Eq 4)}$$

where $\mathrm{SS_T}$ is the total sum of squares, m is the total number of the experiments, and η_i is the S/N ratio at the ith test.

$$\mathrm{SS}_p = \sum_{j=1}^{t} \frac{\left(S_{\eta_j}\right)^2}{t} - \frac{1}{m}\left(\sum_{i=1}^{m} \eta_i\right)^2 \quad \text{(Eq 5)}$$

where SS_p represents the sum of squares from the tested factors, p the one of the tested factors, j the level number of this specific factor p, t the repetition of each level of the factor p, and S_{η_j} the sum of the S/N ratio involving this factor and level j.

$$V_p(\%) = \frac{\mathrm{SS}_p}{\mathrm{D}_p} \times 100 \quad \text{(Eq 6)}$$

where V_p is the variance from the tested factors, and D_p is the degree of freedom for each factor.

Basically, the degrees of freedom (DOF) for the OA should be greater than or at least equal to those for the parameters (Ref 6). For example, a five-level design parameter counts for four DOF. In this study, experimental DOF is 8 (number of trails minus one); while parameters-DOF is 2 (number of parameter levels minus one).

$$\mathrm{SS}'_p = \mathrm{SS}_p - D_p V_\mathrm{e} \quad \text{(Eq 7)}$$

where SS'_p represents the corrected sum of squares from the tested factors and V_e the variance for the error.

$$P_p(\%) = \frac{\mathrm{SS}'_p}{\mathrm{SS_T}} \times 100 \quad \text{(Eq 8)}$$

where P_p is the percentage of the contribution to the total variation of each individual factor.

Table 9 shows the results of ANOVA for hardness. As seen in Table 9, pulse current is the most influencing factor on the hardness of the PCGTAW process with the 73.36% contribution. The second most influencing factor is % on time with 23.54% contribution. Moreover, it was observed that pulse frequency and background current were the insignificant factors with the 2.98 and 0.12% contributions, respectively. In the ANOVA analysis, if the contribution percent is high, the contribution of the factors to that particular response is more. Likewise, lower the contribution percent lower the contribution of the factors on the measured response. Therefore, another analysis is conducted by pooling insignificant factors to error (see Table 10). The process of disregarding an individual factor's contribution and then subsequently adjusting the contribution of the other factor is known as pooling (Ref 29). The results of ANOVA after pooling for hardness are presented in Table 10. Pooled ANOVA values revealed that the pulse current (71.81%) was significant factor for the hardness in the PCGTAW process.

In the case of toughness, ANOVA with the percentage contribution of each factor are shown in Table 11. The pulse current has the greatest influence on the toughness of the PCGTAW process with the 79.18% contribution followed by the background current with 18.81%, the pulse frequency with 1.47% and the % on time with 0.54%. As seen in Table 11, pulse frequency and % on time are insignificant. Table 12 shows the results of ANOVA after pooling for toughness. It can be deduced from above discussions and Table 10 and 12 that the pulse current had the most significant effect on the hardness and the toughness of the PCGTAW process.

4.3 Confirmation Experiment

Once the optimal level of the design parameters is selected, the final step is to predict and verify the improvement of the quality characteristic using the optimal level of the design parameters (Ref 20, 31). The predicted S/N ratio $\left(\hat{\eta}\right)$ using the optimal level of the design parameters can be calculated as (Ref 20):

Table 9 Results of the ANOVA for hardness

Character	Parameters	Degree of freedom (D)	Sum of squares (SS)	Variance (V)	Corrected sums of squares (SS′)	Contribution (P, %)	Rank	Significant
A	Pulse current	2	3304.22	1652.11	3304.22	73.36	1	Yes
B	Background current	2	5.56	2.78	5.56	0.12	4	No
C	% On time	2	1060.22	530.11	1060.22	23.54	2	Yes
D	Pulse frequency	2	134.22	67.11	134.22	2.98	3	No
Error		0	0	0	0	0		
Total		8	4504.22					

Table 10 Pooled ANOVA for hardness

Character	Parameters	Degree of freedom (D)	Sum of squares (SS)	Variance (V)	Corrected sums of squares (SS′)	Contribution (P, %)
A	Pulse current	2	3304.22	1652.11	3234.33	71.81
B	Background current	(2)	(5.56)	Pooled		
C	% On time	2	1060.22	530.11	990.33	21.99
D	Pulse frequency	(2)	(134.22)	Pooled		
Error		4	139.78	34.945		6.2
Total		8	4504.22			100

Table 11 Results of the ANOVA for toughness

Character	Parameters	Degree of freedom (D)	Sum of squares (SS)	Variance (V)	Corrected sums of squares (SS′)	Contribution (P, %)	Rank	Significant
A	Pulse current	2	228.222	114.111	228.222	79.18	1	Yes
B	Background current	2	54.222	27.111	54.222	18.81	2	Yes
C	% On time	2	1.556	0.778	1.556	0.54	4	No
D	Pulse frequency	2	4.222	2.111	4.222	1.47	3	No
Error		0	0	0	0	0		
Total		8	288.222				100	

Table 12 Pooled ANOVA for toughness

Character	Parameters	Degree of freedom (D)	Sum of squares (SS)	Variance (V)	Corrected sums of squares (SS′)	Contribution (P, %)
A	Pulse current	2	228.222	114.111	225.333	78.18
B	Background current	2	54.222	27.111	51.333	17.81
C	% On time	(2)	(1.556)	Pooled		
D	Pulse frequency	(2)	(4.222)	Pooled		
Error		4	5.778	1.4445		4.01
Total		8	288.222			100

$$\widehat{\eta} = \eta_m + \sum_{i=1}^{n} (\overline{\eta_i} - \eta_m) \quad \text{(Eq 9)}$$

where η_m is the total mean S/N ratio, $\overline{\eta_i}$ is the mean S/N ratio at the optimal level, and n is the number of the main design parameters that affect the quality characteristic.

The predicted S/N ratio using the optimal PCGTAW parameters for hardness and toughness can then be obtained and the corresponding hardness and toughness can also be calculated using Eq 3.

Table 13 shows the comparison of the predicted hardness and the toughness with the experimental results using the optimal conditions. There is good agreement between the predicted and the experimental hardness being observed. The increase of the S/N ratio from trial no. 1 (50.2644) as shown in Table 4 to the optimal actual data (50.5009) is 0.24 dB, which means thatthe hardness is increased by about 1.03 times. The comparison of the predicted toughness with the experimental data is also shown in Table 13, where a predicted toughness roughly consistent with the actual results is noted. The increase of the S/N ratio from trial no. 5 (34.9638) as shown in Table 4 to the optimal actual data (36.1236) is 1.16 dB and therefore the toughness value is improved by about 1.14 times. In other words, the experiment results confirm the prior design and analysis for optimizing the PCGTAW parameters. Consequently, hardness and toughness of SDSS welds in the PCGTAW process are significantly improved through the Taguchi method approach. Since optimum conditions deter-

Table 13 Evaluation of the predicted hardness and toughness with the experimental results of the confirmation experiment using the optimal conditions

	Parameters				S/N ratio		Performance values	
	A Pulse current, A	B Background current, A	C % on time	D Pulse frequency, Hz	Prediction	Experiment	Prediction	Experiment
Hardness, HV								
Optimum level	1	3	1	1	50.3128	50.5009	327.8	335
Optimum value	100	70	40	1				
Toughness, J								
Optimum level	2	2	2	3	35.4795	36.1236	59.4	64
Optimum value	120	60	60	5				

mined by Taguchi method in laboratory environment is reproducible in real production environments as well (Ref 17, 32), the findings of this study may be very useful for processing at industrial scale.

5. Conclusions

In this article, the Taguchi design method was used to optimize PCGTAW process parameters to obtain the desired characteristics. Various factors affecting the hardness and the toughness of super duplex stainless steel (SDSS, UNS S32760) welds were analyzed and optimized. Additionally, the ANOVA was used to examine how parameters most significant in the PCGTAW process. According to the pooled ANOVA for hardness, the most important parameters affecting the hardness are pulse current (71.81%) and % on time (21.99%). While, the most effective parameters on the toughness are found to be pulse current (78.18%) and background current (17.81%). As a result, the pulse current was the main parameter affecting the hardness and the toughness of SDSS welds. Moreover, the optimum conditions for hardness were observed at 100 A for pulse current, 70 A for background current, 40 for % on time, and 1 Hz for pulse frequency. In the case of toughness, the experimental results indicated that the optimum conditions are 120 A for pulse current, 60 A for background current, 60 for % on time, and 5 Hz for pulse frequency. Finally, the confirmation experiments were conducted to verify the optimal PCGTAW parameters and the results for both hardness and toughness were in good agreement with the data analyzed using the Taguchi method.

References

1. J.C. Lippold and D.J. Kotecki, *Welding Metallurgy and Weldability of Stainless Steels*, Wiley, New York, 2005
2. S.S.M. Tavares, V.F. Terra, J.M. Pardal, and M.P. Cindra Fonseca, Influence of the Microstructure on the Toughness of a Duplex Stainless Steel UNS S31803, *J. Mater. Sci.*, 2005, **40**, p 145–154
3. M. Yousefieh, M. Shamanian, and A. Saatchi, Influence of Step Annealing Temperature on the Microstructure and Pitting Corrosion Resistance of SDSS UNS S32760 Welds, *J. Mater. Eng. Perform.*, 2011, **20**, p 1678–1683
4. S.S.M. Tavares, J.M. Pardal, L.D. Lima, I.N. Bastos, A.M. Nascimento, and J.A. de Souza, Characterization of Microstructure, Chemical Composition, Corrosion Resistance and Toughness of a Multipass Weld Joint of Superduplex Stainless Steel UNS S32750, *Mater. Charact.*, 2007, **58**, p 610–616
5. International Molybdenum Association, *Practical Guidelines for the Fabrication of Duplex Stainless Steels*, International Molybdenum Association, London, 1999
6. M. Yousefieh, M. Shamanian, and A. Saatchi, Optimization of the Pulsed Current Gas Tungsten Arc Welding (PCGTAW) Parameters for Corrosion Resistance of Super Duplex Stainless Steel (UNS S32760) Welds Using the Taguchi Method, *J. Alloys Compd.*, 2011, **509**, p 782–788
7. S.H. Wang, P.K. Chiu, J.R. Yang, and J. Fang, Gamma (γ) Phase Transformation in Pulsed GTAW Weld Metal of Duplex Stainless Steel, *Mater. Sci. Eng. A*, 2006, **420**, p 26–33
8. A.A. Gokhale, D.J. Tzavaras, H.D, Brody, and G.M. Ecer, *Proceedings of Conference on Grain Refinement in Casting and Welds*, TMS-AIME, St. Louis (MO), 1982, p 223–247
9. P.K. Giridharan and N. Murugan, Optimization of Pulsed GTA Welding Process Parameters for the Welding of AISI, 304L Stainless Steel Sheets, *Int. J. Adv. Manuf. Technol.*, 2009, **40**, p 478–489
10. E. Ozbay, A. Oztas, A. Baykasoglu, and H. Ozbebek, Investigating Mix Proportions of High Strength Self Compacting Concrete by Using Taguchi Method, *Construct. Build. Mater.*, 2009, **23**, p 694–702
11. I. Turkmen, R. Gul, C. Celik, and R. Demirboga, Determination by Taguchi Method of Optimum Conditions for Mechanical Properties of High Strength Concrete with Admixtures of Silica Fume and Blast Furnace Slag, *Civil. Eng. Environ. Syst.*, 2003, **20**(2), p 105–118
12. Z. Beril Gonder, Y. Kaya, I. Vergili, and H. Barlas, Optimization of Filtration Conditions for CIP Wastewater Treatment by Nanofiltration Process Using Taguchi Approach, *Sep. Purif. Technol.*, 2010, **70**, p 265–273
13. M.A. Domínguez-Aguilar and R.C. Newman, Detection of Deleterious Phases in Duplex Stainless Steel by Weak Galvanostatic Polarization in Alkaline Solution, *Corros. Sci.*, 2006, **48**, p 2560–2576
14. J.M. Pardal, S.S.M. Tavares, M. Cindra Fonseca, J.A. de Souza, R.R.A. Côrte, and H.F.G. de Abreu, Influence of the Grain Size on Deleterious Phase Precipitation in Superduplex Stainless Steel UNS S32750, *Mater. Charact.*, 2009, **60**, p 165–172
15. H.P. Klug and L.E. Alexander, *X-ray Diffraction Procedures for Poly Crystalline and Amorphous Materials*, 2nd ed., Wiley, New York, 1974
16. Annual Book of ASTM Standards, Designation E-23-94b, 1995, p 137
17. P.J. Ross, *Taguchi Techniques for Quality Engineering*, McGraw-Hill International Editions, New York, 1988
18. Y. Wang and D.O. Northwood, Optimization of the Polypyrrole-Coating Parameters for Proton Exchange Membrane Fuel Cell Bipolar Plates Using the Taguchi Method, *J. Power Sour.*, 2008, **185**, p 226–232
19. S. Madhav Phadke, *Quality Engineering Using Robust Design*, Prentice Hall, Upper Saddle River, NJ, 1989
20. W.H. Yang and Y.S. Tarng, Design Optimization of Cutting Parameters for Turning Operations Based on the Taguchi Method, *J. Mater. Process. Technol.*, 1998, **84**, p 122–129
21. T.H. Chen and J.R. Yang, Microstructural Characterization of Simulated Heat Affected Zone in a Nitrogen-Containing 2205 Duplex Stainless Steel, *Mater. Sci. Eng. A*, 2002, **338**, p 166–181
22. J.D. Kordatos, G. Fourlaris, and G. Papadimitriou, The Effect of Cooling Rate on the Mechanical and Corrosion Properties of SAF 2205 (UNS 31803) Duplex Stainless Steel Welds, *Scripta Mater.*, 2001, **44**, p 401–408
23. M. Pohl, O. Storz, and T. Glogowski, Effect of Intermetallic Precipitations on the Properties of Duplex Stainless Steel, *Mater. Charact.*, 2007, **58**, p 65–71

24. ASM Speciality Handbook, "Stainless Steels," 1994
25. I. Zucato, M.C. Moreira, I.F. Machado, and S.M.G. Lebrao, Microstructural Characterization and the Effect of Phase Transformations on Toughness of the UNS 31803 Duplex Stainless Steel Aged Treated at 850°C, *Mater. Res.*, 2002, **5**(3), p 385–389
26. R. Badji, M. Bouabdallah, B. Bacroix, C. Kahloun, B. Belkessa, and H. Maza, Phase Transformation and Mechanical Behavior in Annealed 2205 Duplex Stainless Steel Welds, *Mater. Charact.*, 2008, **59**, p 447–453
27. V.S. Moura, L.D. Lima, J.M. Pardal, A.Y. Kina, R.R.A. Corte, and S.S.M. Tavares, Influence of Microstructure on the Corrosion Resistance of the Duplex Stainless Steel UNS S31803, *Mater. Charact.*, 2008, **59**, p 1127–1132
28. J.O. Nilssom, P. Kangas, T. Karlsson, and A. Wilson, Mechanical Properties, Microstructural Stability and Kinetcs of σ Phase Formation in a 29Cr–6Ni–2Mo–0.38N Superduplex Stainless Steel, *Metall. Mater. Trans. A*, 2000, **31**, p 35–45
29. K. Yang, E.C. Teo, and F.K. Fuss, Application of Taguchi Method in Optimization of Cervical Ring Cage, *J. Biomech.*, 2007, **40**, p 3251–3256
30. Y. Ma, H. Hu, D. Northwood, and X. Nie, Optimization of the Electrolytic Plasma Oxidation Processes for Corrosion Protection of Magnesium Alloy AM50 Using the Taguchi Method, *J. Mater. Process. Technol.*, 2007, **182**, p 58–64
31. K.D. Kim, D.N. Han, and H.T. Kim, Optimization of Experimental Conditions Based on the Taguchi Robust Design for the Formation of Nano-Sized Silver Particles by Chemical Reduction Method, *Chem. Eng. J.*, 2004, **104**, p 55–61
32. G. Taguchi, *System of Experimental Design Quality Resources*, Vol 1, Kraus, New York, 1987, p 108–115